RESEARCH PAPER

Nanoscale synthesis of polyoxovanadate organic-inorganic hybrid for naked-eye dopamine detection

Faezeh Moghzi, Janet Soleimannejad *

School of Chemistry, College of Science, University of Tehran, Tehran, Iran

ARTICLE INFO

Article History:
Received 26 June 2021
Accepted 12 September 2021
Published 1 May 2022

Keywords:
Organic-inorganic hybrid
Polyoxovanadates
Nanomaterials
Optical sensing
Dopamine

ABSTRACT

Decavanadate based compounds as a class of polyoxometalates family are known for their wide range of applications in chemical, biological, and physical sciences. Considering the size-dependent chemical properties of polyoxometalates and the unique properties of decavanadates, the nanoscale $(HNic)_6[V_{10}O_{28}].H_2O$ (**1**), an organic-inorganic hybrid compound was synthesized using ultrasound and in the presence of a weak solvent. The nanostructures were characterized by FT-IR spectroscopy, powder X-ray diffraction (PXRD), scanning electron microscopy (SEM), energy dispersive X-ray spectroscopy (EDS), and elemental analysis. The results showed that by increasing the amount of the weak solvent, the size and crystallinity of nanoparticles decreased. Optical studies revealed a green emission with a maximum at 530 nm from nanoscale 1 which is assigned to O→V charge transfer transition and it was used for dopamine (DA) detection. Interestingly, nanoscale 1 catalyzed the in-situ formation of polydopamine nanoparticles, the formation of which decreased the fluorescence intensity of nanoscale 1 which was successfully utilized for naked-eye dopamine molecules detection.

How to cite this article
Moghzi F., Soleimannejad J. Nanoscale synthesis of polyoxovanadate organic-inorganic hybrid for naked-eye dopamine detection. Nanochem Res, 2022; 7(1):1-8. DOI: 10.22036/ncr.2022.01.001

INTRODUCTION

Polyoxometalates (POMs), as a series of anionic metal-oxo clusters of Mo, W, V, Nb, and Ta, are generally utilized as building blocks to construct nano- or micro-materials. Because of their abundant structure and distinct properties, the studies of POMs are of particular interest in a wide variety of disciplines, such as catalysis, electrochemistry, biochemistry, optical and material engineering [1-8]. As a branch of POMs, polyoxovanadates (POVs) play an important role in POM chemistry. The decavanadate anions $[H_nV_{10}O_{28}]^{(6-n)-}$ are one of the dominant vanadium oxoanions present in an aqueous solution. Many crystal structures of simple inorganic decavanadates and associated with organic counterions have been reported so far [9, 10]. For example, both the heterocyclic organic ligands and charge transfer can introduce photoluminescence properties to the POM systems. Until now, several inorganic POVs incorporating decavanadate $[V_{10}O_{28}]^{6-}$ structures have been shown to act as efficient luminescent probes because of their satisfactory luminescence behaviors derived from O→V charge transfer [11-15]. Among the dazzling detection technologies, fluorescence detection has been becoming a feasible operation due to its high selectivity, convenience, rapid response, facile operation, and so forth [16].

Nanomaterials in the form of nanoparticles, nanofilms, nanocomposites, and nanoflakes have been used for various purposes, such as improved sensing abilities [17-22]. In recent years, the synthesis and characterization of nanomaterials have received attention owing to their size-

* Corresponding Author Email: *janet_soleimannejad@khayam.ut.ac.ir*

dependent chemical and physical properties [23, 24]. It has been confirmed that nanoscale POMs are more effective than bulk materials in particular sensing applications [25, 26]. Several methods have been developed to prepare nanoscale materials, among which the sonochemical synthesis presents a simple, environmentally green, efficient, and inexpensive platform. Ultrasonic irradiation provides a nanoreactor for the facile synthesis of nanomaterials along short reaction times [27, 28].

Dopamine is known as a biomarker for numerous diseases such as schizophrenia, epilepsy, Parkinson's, and memory loss [29]. The optical sensing of dopamine molecules for the diagnosis of such diseases has attracted much attention as a simple methodology due to its easy-to-use, fast response, and cost-efficiency [29]. In this study, we synthesized an organic-inorganic hybrid compound based on polyoxovanadate $(HNic)_6[V_{10}O_{28}].H_2O$ (**1**). The nanoscale **1** was prepared under ultrasonic irradiation and was fully characterized. The optical properties of **1** were investigated and the green emission of these nanoparticles with a maximum at 530 nm was utilized for naked-eye DA detection.

EXPERIMENTAL METHOD

Materials and methods

Reagents used in this work were consumed without further purification. The ultrasonic syntheses were carried out on a SONIC 3MX with the power of 160W. The FT-IR spectra of **1** were recorded by utilizing a Bruker Enquinox 55 spectrometer with KBr pellet in the range of 400-4000 cm^{-1}. Powder X-ray diffraction (PXRD) measurements were performed using a PANalytical X'Pert PRO MRD equipped with a CuKα radiation source (λ = 1.54184 Å). SEM images were obtained with a FEI Quanta 650F microscope with a beam voltage of 20 kV. The absorption spectra of the organic solutions and water suspensions were registered in the Agilent Cary 60 spectrophotometer using a 1x1 cm quartz cuvette. The emission spectra of nanoscale **1** were recorded through the PTI QuantaMaster 300 phosphorescence/ fluorescence spectrophotometer (Horiba Ltd.). Energy Dispersive X-ray Spectroscopy (EDS) was coupled with FEI Quanta 650F microscope.

A deep yellow single crystal of **1** was selected to collect data on a four-circle KUMA KM4 diffractometer with a two-dimensional CCD area detector. The graphite monochromatized MoKα radiation (λ = 0.71073 Å) and the ω-scan technique (Δω = 1°) were applied for data collection. Data collection and reduction, along with absorption correction, were accomplished via the CrysAlis software package [30]. The structure was solved by direct methods using SHELXT [31] giving positions of almost all non-hydrogen atoms. The other atoms were S3 localized with subsequent difference Fourier syntheses. The structure was refined using SHELXL-2018 [31] with anisotropic thermal displacement parameters. The data were deposited in Cambridge crystallographic data center with deposition number CCDC 1824532.

Synthesis of $(HNic)_6[V_{10}O_{28}].H_2O$

Twenty ml aqueous solution of $VOSO_4.5H_2O$ (0.5 mmol, 125 mg) was mixed with 10 ml aqueous solution of nicotinamide (1 mmol, 122 mg), and the resultant solution was refluxed for four hours. The final mixture was cooled down to room temperature and precipitates were filtered. The single crystals of **1** were grown through slow evaporation of filtered solution after two days. (yield 72%), m.p. > 300 °C. Anal. Calcd for $V_{10}O_{28}{\cdot}6(C_6H_7N_2O).2(H_2O)$: C 24.93, H 2.65, N 9.69%. Found: C 25.32, H 2.51, N 10.01%.

Synthesis of nanoscale $(HNic)_6[V_{10}O_{28}].H_2O$

For the synthesis of nanoscale **1**, two strategies were applied simultaneously, including utilizing weak solvent and operating ultrasonic irradiation. To prepare nanoscale $(HNic)_6[V_{10}O_{28}].H_2O$, an aqueous solution of $VOSO_4.5H_2O$ (15 ml, 0.05M) was positioned in an ultrasonic bath. A solution of nicotinamide (30 ml 0.05M) in a water/ethanol mixture with a 1:1 volume ratio was added dropwise to the above solution. The mixture was irradiated for 1h with a maximum power output of 160 W. To investigate the effect of weak solvent addition, the water/ethanol volume ratio was changed from 1:1 to 1:2.

Naked-eye DA detection

A stable suspension (1mg/ml) was prepared by floating nanoscale **1** into distilled water under ultrasonic irradiation (10 min). For DA detection 2ml of the formed suspension was mixed with dopamine solutions (2ml) with different concentrations from 1 to 30 μM. Subsequently, the color changes were recorded.

For the paper test, the cellulose paper was cut into a 20 cm × 12 mm strip. One hundred microliters of the nanoscale **1** suspension were drop-casted

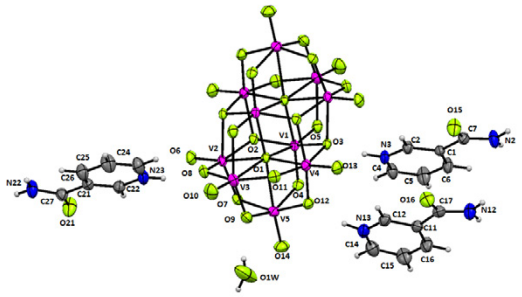

Fig. 1 View $(HNic)_6[V_{10}O_{28}].H_2O$ (**1**) with the anisotropic displacement parameters. The labelling scheme of the atoms is shown only in the asymmetric unit.

onto the strip and dried in a vacuum chamber for 3h, and afterward circles (diameter ≈1cm) were cut from the strip. Then 10 µl of the various dopamine concentrations were pipetted on top of the circles. The fluorescence intensity changes were recorded in a dark box using a UV lamp, excited at 365 nm.

RESULTS AND DISCUSSION

Crystal structure of $(HNic)_6[V_{10}O_{28}].H_2O$

$(HNic)_6[V_{10}O_{28}].H_2O$ (**1**) is crystallized in the monoclinic system with space group *C*2/c (Table S1). The crystal structure of compound **1** is similar to the previously reported structure which had been synthesized with more precursors and a complicated route [32]. The asymmetric unit consists of three crystallographically independent mono-protonated nicotinamide cations ($HNic^+$), one half-decavanadate anion, and a water molecule (Fig. 1a). Each water molecule is a bridge between two decavanadate anions through O1*W*–H1*W*···O9 and O1*W*–H2*W*···O7^v hydrogen bondings. The decavanadate cluster can be presented as a polyoxometalate with three different types of vanadium atoms (Fig S1). Six vanadium atoms are located in a plan (V_b and V_c) and four vanadium atoms are present on both sides of the plan (V_a). The 28 oxygen atoms are coordinated to vanadium atoms through six to form $[V_{10}O_{28}]^{6-}$ cluster. The oxygen atoms in decavanadate are classified into four types including μ_6, μ_3, μ_2, and terminal coordination modes. Six $HNic^+$ cations are connected to the decavanadate anion through the hydrogen bonding between protonated pyridine rings and terminal coordinated oxygen of polyoxometalate anions (Fig. 2). Moreover, protonated nicotinamide is connected via hydrogen bonding among amide groups. Therefore, noncovalent interactions such as N–H···O3, O–H···O hydrogen bonding with

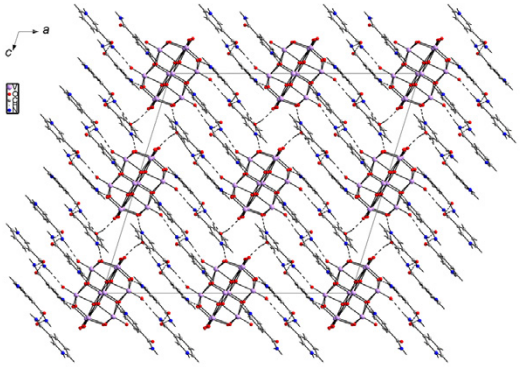

Fig. 2 Supramolecular architecture of compound **1** along *b*-axis (dashed lines represent the O-H..O and N-H…O hydrogen bonds)

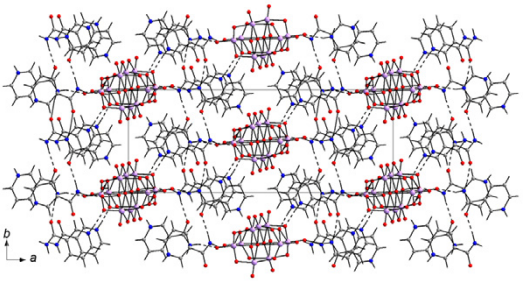

Fig. 3 The packing structure of compound **1** derived from π-π interactions and hydrogen bonds along *c*-axis.

D···A interaction distance ranging from 2.570(2) Å to 2.852(2) Å, and ion-pairing interaction between $[V_{10}O_{28}]^{6-}$ and $HNic^+$ have a key role in the supramolecular architecture of compound **1**. The details of hydrogen bonding are presented in Table S2. Furthermore, in the supramolecular packing of compound **1**, there are π-π interactions between pyridine rings with interaction distances ranging from 3.510 to 3.624 Å (Fig. 3).

Sonochemical synthesis, morphology, and chemical stability

The nanostructures of **1** were synthesized under ultrasonic irradiation with different volumes of weak solvent. The bulk crystals of **1** are partially soluble in water and completely insoluble in ethanol. Thus, ethanol was selected as a weak solvent for the sonochemical synthesis of nanoscale **1**. The morphology of bulk crystals and their nanostructures were studied using SEM images. As shown in Fig. 4, the bulk crystals of **1** have octahedral morphologies. The SEM images of nanoscale **1**, with 1:1 ethanol to water volume ratio, demonstrate a monodispersed distribution of nanoparticles with octahedral morphologies

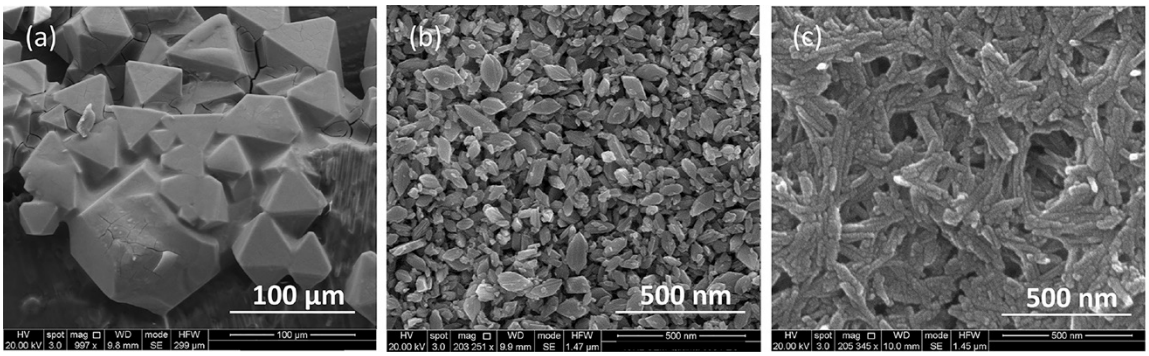

Fig. 4 (a) SEM image of compound **1**, (b) and (c) SEM images of nanoscale **1** formed by different ethanol/water volume ratio including 1:1 and 2:1.

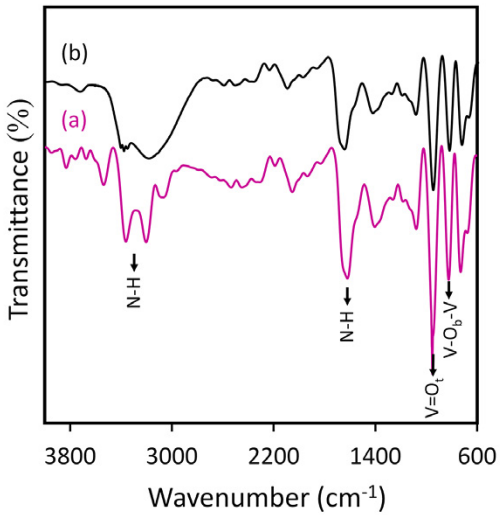

Fig. 5 FT-IR spectra of compound **1** as (a) bulk crystals and (b) nanoparticles produced by sonochemical method.

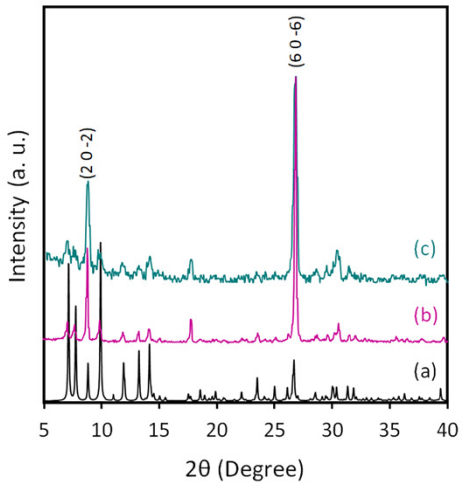

Fig. 6 (a) The simulated pattern based on single-crystal X-ray diffraction data of **1**, XRD patterns of nanoscale **1** formed by different water to ethanol volume ratios: (b) 1:1 and (c) 1:2.

similar to those found for the bulk crystals (Fig. 4b). It is evident from Fig. 4c that by increasing the volume ratio of ethanol to water, the size and crystallinity of nanoparticles are decreased.

The FT-IR spectroscopy was utilized to corroborate the functional groups of bulk crystals and the chemical stability of nanoscale **1**. As presented in Fig. 5a, the infrared spectrum of **1** shows that the N–H vibration peaks at 3200-3400 and 1618 cm^{-1} can be ascribed to the amide and protonated pyridyl groups. The characteristic bond of V=O symmetric vibration (terminal coordination mode in decavanadate cluster) at 950 cm^{-1} and the presence of the V-O-V bridging vibration bond at 819 cm^{-1} confirm the formation of decavanadate cluster. The FTIR spectrum of nanoscale **1** is compatible with the FT-IR spectrum of bulk crystals indicating the chemical stability of these nanoparticles (Fig. 5b).

The comparison between the PXRD patterns of the nanoscale **1** and the simulated pattern of single crystals' XRD confirms the single-phase purity of nanoscale **1** (Fig. 6). In addition, as mentioned before, these patterns indicate that the crystallinity of nanoscale **1** is decreased by increasing the amount of ethanol and some peaks are eliminated from the PXRD pattern (Fig. 6c).

Optical properties and naked-eye dopamine detection

To study the optical properties of nanoscale **1**, the UV-Vis absorption spectrum of this compound was recorded from 200 to 700 nm (Fig. 7a). The absorption band observed around 230 nm can be

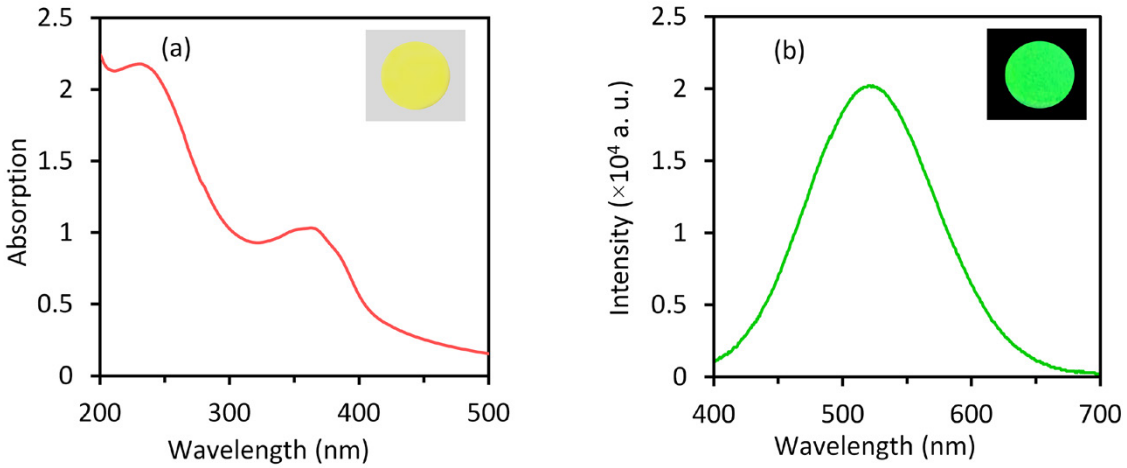

Fig. 7 (a) Absorption spectra of nanoscale **1** and (b) emission spectra of nanoscale **1** upon a 365 nm excitation.

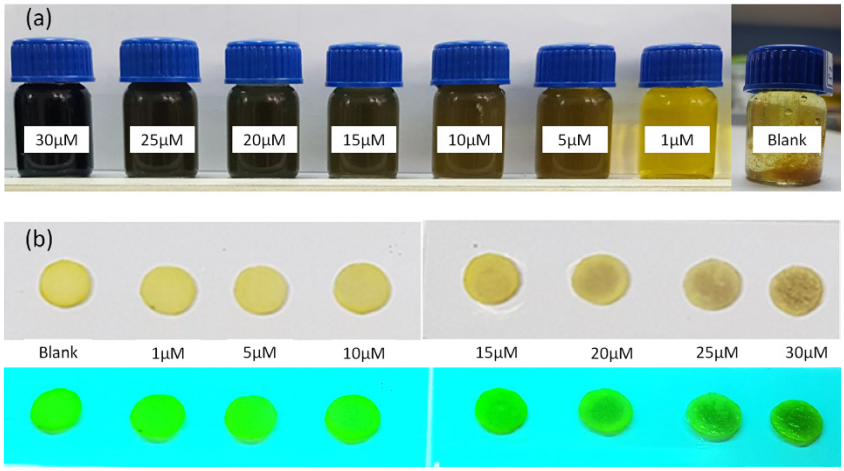

Fig. 8 (a) The photographs show the color change of nanoscale **1** suspensions after adding different concentrations of DA molecules (b) The photographs of the paper strips in the presence of various amounts of DA under sunlight and a 365 nm UV lamp.

ascribed to π-π* of nicotinamide and the band with a maximum at 360 nm can be assigned to π(O)→d(V) charge transfer transitions. The luminescence behaviors derived from O→V charge transfer were investigated upon a 365 nm excitation. The solid-state fluorescence of nanoscale **1** upon a 365 nm excitation exhibited a broad band with green emission (Fig. 7b).

To assess the capability of nanoscale **1** for DA detection, the optical properties of these nanoparticles in the presence of different concentrations of dopamine molecules were investigated. As shown in Fig.8a, polydopamine formation is observed as a color change from yellow to black by mixing dopamine solutions and suspensions of nanoscale **1**. According to previous studies, vanadium can catalyze dopamine oxidation [33]. The mechanism of polydopamine formation is shown in scheme 1[34]. In situ formation of polydopamine was observed in the presence of nanoscale **1**. The oxidation and polymerization of dopamine were very fast and a stable suspension of polydopamine was formed. Visual DA detection based on a paper test strip was performed by a UV lamp at 365 nm excitation wavelength. It is evident from Fig. 8b that polydopamine formation can quench the emission of nanoscale **1** and fluorescence intensity changes can be easily recognized by naked-eye at different DA concentrations.

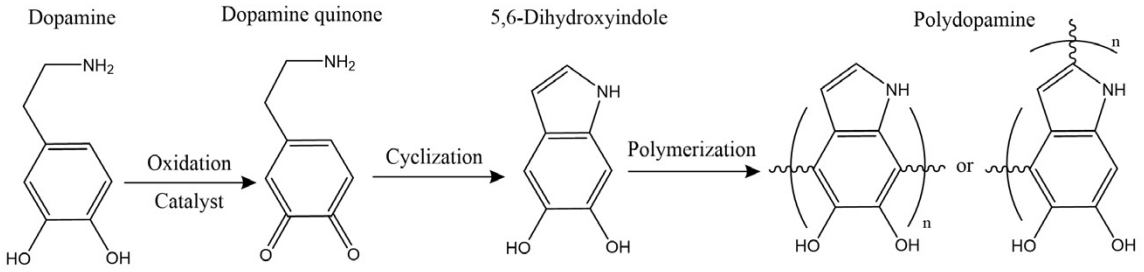

Scheme 1. The mechanism of polydopamine formation [34].

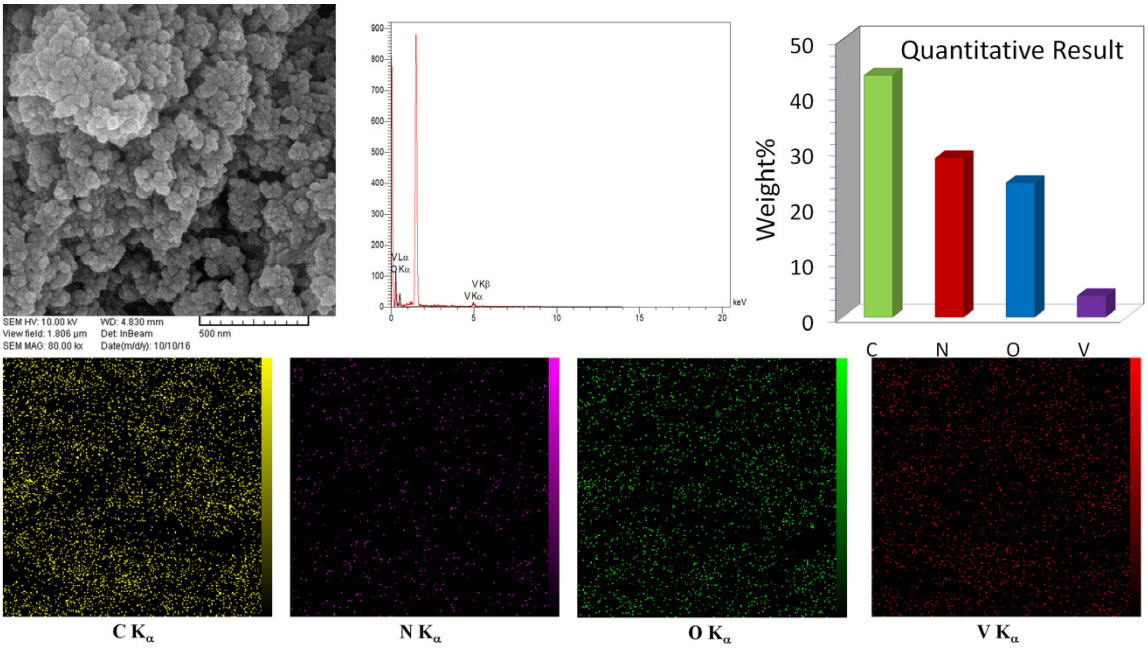

Fig. 9 SEM, EDS, and mapping of nanoscale **1**@polydopamine.

To clarify the mechanism of DA detection, the suspensions of nanoscale **1** were centrifuged (2000 rpm) for 5 min in the presence of DA molecules, and the black precipitates were separated from the suspensions. Energy Dispersive X-Ray spectroscopy was utilized to analyze the chemical composition of black precipitates (Fig. 9). The mass ratios of C, N, and O to V confirm the formation of polydopamine nanoparticles on the surface of nanoscale **1**. As presented in scheme **1**, the first step of polydopamine formation is an oxidation reaction that requires a catalyst to accelerate the oxidation of dopamine and the other steps are spontaneous [35, 36]. In several studies, the catalysis capability of decavanadate for oxidation reactions has been confirmed [37-39]. The formation of polydopamine was examined in the absence of nanoscale **1** and the *in situ* formation of black precipitate was not observed. In addition, polydopamine formation can quench the fluorescence of nanoscale **1** due to a large molecular network of polydopamine [40]. These results confirm the catalysis capability of compound **1** for the polydopamine formation and the quenching mechanism of fluorescence intensity in the presence of DA molecules.

CONCLUSION

Nanostructures of $(HNic)_6[V1_0O_{28}].H_2O$ were prepared using two strategies including utilizing a weak solvent and operating ultrasonic irradiation. The results reveal a direct correlation between the volume of the weak solvent and the size of nanoscale **1**. Additionally, the optical properties of compound **1** were investigated and

the green fluorescence of nanoscale **1** upon a 365 nm excitation can be assigned to π(O)→d(V) charge transfer transitions. Nanoparticles of **1** have shown to be an efficient nano-catalyst for dopamine oxidation and polydopamine formation. The formation of polydopamine nanoparticles was very fast and it quenched the green fluorescence of nanoscale **1**; this capability was used for naked-eye dopamine detection.

CONFLICTS OF INTEREST

The authors declare that there are no conflicts of interest regarding the publication of this paper.

REFERENCES

[1] Li J-K, Wei C-P, Wang Y-Y, Zhang M, Lv X-R, Hu C-W. Conversion of V_6 to V_{10} cluster: Decavanadate-based Mn-polyoxovanadate as robust heterogeneous catalyst for sulfoxidation of sulfides. Inorganic Chemistry Communications. 2018;87:5-7. https://doi.org/10.1016/j.inoche.2017.11.009

[2] Liu J, Han Q, Chen L, Zhao J. A brief review of the crucial progress on heterometallic polyoxotungstates in the past decade. CrystEngComm. 2016;18(6):842-62. https://doi.org/10.1039/C5CE02378E

[3] Oms O, Dolbecq A, Mialane P. Diversity in structures and properties of 3d-incorporating polyoxotungstates. Chemical Society Reviews. 2012;41(22):7497-536. **https://doi.org/10.1039/C2CS35148J**

[4] Cao J-P, Shen F-C, Luo X-M, Cui C-H, Lan Y-Q, Xu Y. Proton conductivity resulting from different triazole-based ligands in two new bifunctional decavanadates. RSC Advances. 2018;8(33):18560-6.

[5] Ma P, Hu F, Wang J, Niu J. Carboxylate covalently modified polyoxometalates: From synthesis, structural diversity to applications. Coordination Chemistry Reviews. 2019;378:281-309.

[6] Song Y-F, Tsunashima R. Recent advances on polyoxometalate-based molecular and composite materials. Chemical Society Reviews. 2012;41(22):7384-402.

[7] Wu H, Ma T, Wu C, Yan L, Su Z. Effect of polyoxometalate in organic-inorganic hybrids on charge transfer and absorption spectra towards sensitizers. Dyes and Pigments. 2017;142:379-86.

[8] Farzaneh F, Moghzi F. Investigation of the catalytic behavior of a Cu coordination polymer capped polyoxometalate as an oxidation catalyst. Reaction Kinetics, Mechanisms and Catalysis. 2015;115(1):175-85.

[9] Hayashi Y. Hetero and lacunary polyoxovanadate chemistry: Synthesis, reactivity and structural aspects. Coordination Chemistry Reviews. 2011;255(19):2270-80.

[10] Amanchi SR, Das SK. A Versatile Polyoxovanadate in Diverse Cation Matrices: A Supramolecular Perspective. Frontiers in Chemistry. 2018;6(469).

[11] Tiago T, Aureliano M, Gutiérrez-Merino C. Decavanadate Binding to a High Affinity Site near the Myosin Catalytic Centre Inhibits F-Actin-Stimulated Myosin ATPase Activity. Biochemistry. 2004;43(18):5551-61.

[12] Lü Y, Feng Y. A Potassium-Lithium Double Salt of Decavanadate Showing Unprecedented (6,8)-Connected Topology. Chinese Journal of Chemistry. 2010;28(12):2404-10.

[13] Yerra S, Tripuramallu BK, Das SK. Decavanadate-based discrete compound and coordination polymer: Synthesis, crystal structures, spectroscopy and nano-materials. Polyhedron. 2014;81:147-53.

[14] Sedgwick MA, Crans DC, Levinger NE. What Is Inside a Nonionic Reverse Micelle? Probing the Interior of Igepal Reverse Micelles Using Decavanadate. Langmuir. 2009;25(10):5496-503.

[15] Sedghiniya S, Soleimannejad J, Jahani Z, Davoodi J, Janczak J. Crystal engineering of an adenine-decavanadate molecular device towards label-free chemical sensing and biological screening. Acta Crystallographica Section B. 2020;76(1):85-92.

[16] Borisov SM, Wolfbeis OS. Optical Biosensors. Chemical Reviews. 2008;108(2):423-61.

[17] Arduini F, Cinti S, Scognamiglio V, Moscone D. 13 - Nanomaterial-based sensors. In: Mustansar Hussain C, editor. Handbook of Nanomaterials in Analytical Chemistry: Elsevier; 2020. p. 329-59.

[18] Holzinger M, Le Goff A, Cosnier S. Nanomaterials for biosensing applications: a review. Frontiers in Chemistry. 2014;2(63).

[19] Krishnan SK, Singh E, Singh P, Meyyappan M, Nalwa HS. A review on graphene-based nanocomposites for electrochemical and fluorescent biosensors. RSC Advances. 2019;9(16):8778-881.

[20] Vasilescu A, Gheorghiu M, Peteu S. Nanomaterial-based electrochemical sensors and optical probes for detection and imaging of peroxynitrite: a review. Microchimica Acta. 2017;184(3):649-75.

[21] Zheng Y, Sun F-Z, Han X, Xu J, Bu X-H. Recent Progress in 2D Metal-Organic Frameworks for Optical Applications. Advanced Optical Materials. 2020;8(13):2000110.

[22] Moghzi F, Soleimannejad J, Janczak J. Dual-emitting barium based metal-organic nanosheets as a potential sensor for temperature and anthrax biomarkers. Nanotechnology. 2020;31(24):245706.

[23] Kolahalam LA, Kasi Viswanath IV, Diwakar BS, Govindh B, Reddy V, Murthy YLN. Review on nanomaterials: Synthesis and applications. Materials Today: Proceedings. 2019;18:2182-90.

[24] Baig N, Kammakakam I, Falath W. Nanomaterials: a review of synthesis methods, properties, recent progress, and challenges. Materials Advances. 2021;2(6):1821-71.

[25] Wang Y, Weinstock IA. Polyoxometalate-decorated nanoparticles. Chemical Society Reviews. 2012;41(22):7479-96.

[26] Lu F, Wang M, Li N, Tang B. Polyoxometalate-Based Nanomaterials Toward Efficient Cancer Diagnosis and Therapy. Chemistry – A European Journal. 2021;27(21):6422-34.

[27] Contreras-Pereda N, Moghzi F, Baselga J, Zhong H, Janczak J, Soleimannejad J, et al. Ultrasound-assisted exfoliation of a layered 2D coordination polymer with HER electrocatalytic activity. Ultrasonics Sonochemistry. 2021;70:105292.

[28] Moghzi F, Soleimannejad J. Sonochemical synthesis of a new nano-sized barium coordination polymer and its application as a heterogeneous catalyst towards sono-synthesis of biodiesel. Ultrasonics Sonochemistry. 2018;42:193-200.

[29] Moghzi F, Soleimannejad J, Sañudo EC, Janczak J.

Dopamine Sensing Based on Ultrathin Fluorescent Metal–Organic Nanosheets. ACS Applied Materials & Interfaces. 2020;12(40):44499-507.
[30] CrysAlis C. CrysAlis Red 1.171. 38.43. Rigaku Oxford Diffraction. 2015.
[31] Sheldrick G. Crystal structure refinement with SHELXL. Acta Crystallographica Section C. 2015;71(1):3-8.
[32] Pacigova S, Rakovsky E, Sivak M, Zak Z. Hexakis[3-(aminocarbonyl)pyridinium] decavanadate(V) dihydrate. Acta Crystallographica Section C. 2007;63(9):m419-m22.
[33] Langeslay RR, Kaphan DM, Marshall CL, Stair PC, Sattelberger AP, Delferro M. Catalytic Applications of Vanadium: A Mechanistic Perspective. Chemical Reviews. 2019;119(4):2128-91.
[34] Zhao XG, Hwang K-J, Lee D, Kim T, Kim N. Enhanced mechanical properties of self-polymerized polydopamine-coated recycled PLA filament used in 3D printing. Applied Surface Science. 2018;441:381-7.
[35] Gao ZF, Wang XY, Gao JB, Xia F. Rapid preparation of polydopamine coating as a multifunctional hair dye. RSC Advances. 2019;9(35):20492-6.
[36] Parnell CM, Chhetri B, Brandt A, Watanabe F, Nima ZA, Mudalige TK, et al. Polydopamine-Coated Manganese Complex/Graphene Nanocomposite for Enhanced Electrocatalytic Activity Towards Oxygen Reduction. Scientific Reports. 2016;6(1):31415.
[37] Martín-Caballero J, San José Wéry A, Reinoso S, Artetxe B, San Felices L, El Bakkali B, et al. A Robust Open Framework Formed by Decavanadate Clusters and Copper(II) Complexes of Macrocyclic Polyamines: Permanent Microporosity and Catalytic Oxidation of Cycloalkanes. Inorganic Chemistry. 2016;55(10):4970-9.
[38] Buvailo HI, Pavliuk MV, Makhankova VG, Kokozay VN, Bon V, Mijangos E, et al. Facile one-pot synthesis of hybrid compounds based on decavanadate showing water oxidation activity. Inorganic Chemistry Communications. 2020;119:108111.
[39] Gu J, Liu M, Xun S, He M, Wu L, Zhu L, et al. Lipophilic decavanadate supported by three-dimensional porous carbon nitride catalyst for aerobic oxidative desulfurization. Molecular Catalysis. 2020;483:110709.
[40] Yu L, Feng L, Xiong L, Li S, Xu Q, Pan X, et al. Multifunctional nanoscale lanthanide metal–organic framework based ratiometric fluorescence paper microchip for visual dopamine assay. Nanoscale. 2021;13(25):11188-96.